

Nearly transparent SBS slow light in an optical fiber

Zhaoming Zhu and Daniel J. Gauthier

Department of Physics and The Fitzpatrick Institute for Photonics, Duke University, Durham,
NC 27708, USA

zzhu@phy.duke.edu

Abstract: Slow-light delay via stimulated Brillouin scattering (SBS) in optical fibers is usually achieved with delay-dependent amplification that degrades system performance. To address this problem, we propose a SBS slow-light method that makes use of two widely separated anti-Stokes absorption resonances, and achieve nearly transparent slow light in an optical fiber. We demonstrate the method in a highly nonlinear optical fiber, and achieve a slow-light bandwidth of ~ 150 MHz and a relative delay of ~ 0.3 for ~ 9 -ns pulses with a signal attenuation of ~ 4.8 dB.

© 2006 Optical Society of America

OCIS codes: (999.9999) Slow light; (290.5900) Scattering, stimulated Brillouin; (060.5530) Pulse propagation and solitons; (060.4370) Nonlinear optics, fibers

References and links

1. R. W. Boyd and D. J. Gauthier, in *Progress in Optics*, E. Wolf, Ed. (Elsevier, Amsterdam, 2002), Vol. 43, Ch. 6, pp. 497–530.
2. D. Gauthier, “Slow light brings faster communication,” *Phys. World* **18**, 30–32, December 2005.
3. D. J. Gauthier, A. L. Gaeta, and R. W. Boyd, “Slow Light: From basics to future prospects,” *Photonics Spectra*, 44–50, March 2006.
4. R. W. Boyd, D. J. Gauthier, and A. L. Gaeta, “Applications of slow-light in telecommunications,” *Optics & Photonics News*, 19–23, April 2006.
5. L. V. Hau, S. E. Harris, Z. Dutton, and C. H. Behroozi, “Light speed reduction to 17 meters per second in an ultracold atomic gas,” *Nature* **397**, 594 (1999).
6. M. M. Kash, V. A. Sautenkov, A. S. Zibrov, L. Hollberg, G. R. Welch, M. D. Lukin, Y. Rostovtsev, E. S. Fry, and M. O. Scully, “Ultraslow group velocity and enhanced nonlinear optical effects in a coherently driven hot atomic gas,” *Phys. Rev. Lett.* **82**, 5229 (1999).
7. A. V. Turukhin, V. S. Sudarshanam, M. S. Shahriar, J. A. Musser, B. S. Ham, and P. R. Hemmer, “Observation of ultraslow and stored light pulses in a solid,” *Phys. Rev. Lett.* **88**, 023602 (2002).
8. M. S. Bigelow, N. N. Lepeshkin, and R. W. Boyd, “Observation of ultraslow light propagation in a ruby crystal at room temperature,” *Phys. Rev. Lett.* **90**, 113903 (2003).
9. P.-C. Ku, F. Sedgwick, C. J. Chang-Hasnain, P. Palinginis, T. Li, H. Wang, S.-W. Chang, and S.-L. Chuang, “Slow light in semiconductor quantum wells,” *Opt. Lett.* **29**, 2291–2293 (2004).
10. X. Zhao, P. Palinginis, B. Pesala, C. Chang-Hasnain, and P. Hemmer, “Tunable ultraslow light in vertical-cavity surface-emitting laser amplifier,” *Opt. Express* **13**, 7899–7904 (2005).
11. Y. Okawachi, M. S. Bigelow, J. E. Sharping, Z. Zhu, A. Schweinsberg, D. J. Gauthier, R. W. Boyd, and A. L. Gaeta, “Tunable all-optical delays via Brillouin slow light in an optical fiber,” *Phys. Rev. Lett.* **94**, 153902 (2005).
12. K. Y. Song, M. G. Herráez, and L. Thévenaz, “Observation of pulse delaying and advancement in optical fibers using stimulated Brillouin scattering,” *Opt. Express* **13**, 82–88 (2005).
13. K. Y. Song, M. G. Herráez, and L. Thévenaz, “Long optically controlled delays in optical fibers,” *Opt. Lett.* **30**, 1782–1784 (2005).
14. M. G. Herráez, K. Y. Song, and L. Thévenaz, “Optically controlled slow and fast light in optical fibers using stimulated Brillouin scattering,” *Appl. Phys. Lett.* **87**, 081113 (2005).
15. M. G. Herráez, K. Y. Song, and L. Thévenaz, “Arbitrary-bandwidth Brillouin slow light in optical fibers,” *Opt. Express* **14**, 1395–1400 (2006).

16. J. E. Sharping, Y. Okawachi, and A. L. Gaeta, "Wide bandwidth slow light using a Raman fiber amplifier," *Opt. Express* **13**, 6092–6098 (2005).
17. D. Dahan and G. Eisenstein, "Tunable all optical delay via slow and fast light propagation in a Raman assisted fiber optical parametric amplifier: a route to all optical buffering," *Opt. Express* **13**, 6234–6249 (2005).
18. Y. A. Vlasov, M. O'Boyle, H. F. Hamann, and S. J. McNab, "Active control of slow light on a chip with photonic crystal waveguides," *Nature* **438**, 65–69 (2005).
19. H. Gersen, T. J. Karle, R. J. P. Engelen, W. Bogaerts, J. P. Korterik, N. F. van Hulst, T. F. Krauss, and L. Kuipers, "Real-space observation of ultraslow light in photonic crystal waveguides," *Phys. Rev. Lett.* **94**, 073903 (2005).
20. Y. Okawachi, M. Foster, J. Sharping, A. Gaeta, Q. Xu, and M. Lipson, "All-optical slow-light on a photonic chip," *Opt. Express* **14**, 2317–2322 (2006).
21. H. Tanaka, H. Niwa, K. Hayami, S. Furue, K. Nakayama, T. Kohmoto, M. Kunitomo, and Y. Fukuda, "Propagation of optical pulses in a resonantly absorbing medium: Observation of negative velocity in Rb vapor," *Phys. Rev. A* **68**, 053801 (2003).
22. R. M. Camacho, M. V. Pack, and J. C. Howell, "Low-distortion slow light using two absorption resonances," *Phys. Rev. A* **73**, 063812 (2006).
23. M. Nikles, L. Thévenaz, and P. A. Robert, "Brillouin gain spectrum characterization in single-mode optical fibers," *J. Lightwave Technol.* **15**, 1842–1851 (1997).
24. M. D. Stenner, M. A. Neifeld, Z. Zhu, A. M. C. Dawes, and D. J. Gauthier, "Distortion management in slow-light pulse delay," *Opt. Express* **13**, 9995–10002 (2005).
25. Z. Zhu, D. J. Gauthier, Y. Okawachi, J. E. Sharping, A. L. Gaeta, R. W. Boyd, and A. E. Willner, "Numerical study of all-optical slow-light delays via stimulated Brillouin scattering in an optical fiber," *J. Opt. Soc. Am. B* **22**, 2378–2384 (2005).
26. R. Pant, M. D. Stenner, M. A. Neifeld, Z. Shi, R. W. Boyd, and D. J. Gauthier, "Maximizing the opening of eye diagrams for slow-light systems," submitted for publication, 2006.
27. B. Macke and B. Segard, "Pulse normalization in slow-light media," *Phys. Rev. A* **73**, 043802 (2006).
28. Z. Zhu, A. M. C. Dawes, D. J. Gauthier, L. Zhang, and A. E. Willner, "12-GHz-bandwidth SBS slow light in optical fibers," *Optical Fiber Conference 2006*, paper PDP1.
29. Z. Zhu, A. M. C. Dawes, D. J. Gauthier, L. Zhang, and A. E. Willner, "Broadband SBS slow light in an optical fiber," submitted to *J. Lightwave Technol.* (2006).

1. Introduction

There has been a great deal of interest in slow light, in which the propagation speed of light pulses is controllably slowed down [1]. Slow light has potential applications in optical buffering, data synchronization, optical memories, and optical signal processing [2-4]. Most slow light techniques rely on resonant effects that cause large normal dispersion in a narrow spectral region (approximately equal to the resonance width), which increases the group index and thus reduces the group velocity of optical pulses. Slow light has been demonstrated in various materials including atomic gases [5, 6], solid crystals [7, 8], semiconductors [9, 10], optical fibers [11-17], and other photonic structures [18-20]. In particular, slow light in optical fibers has recently attracted a lot of interest due to the inherent advantages with optical fibers such as compatibility with fiber-optic communication systems, room temperature operation, and the potential for large bandwidths. Slow light in optical fibers has been demonstrated via optical amplifying resonances associated with stimulated Brillouin scattering (SBS) [11-15], stimulated Raman scattering [16], and parametric amplification [17]. In these fiber-based slow-light methods, pulse delay is achieved via an amplification resonance, where the delay is proportional to the exponential gain coefficient associated with the resonance. Thus, the intensity of the data pulse passing through the slow-light channel experiences large variation in a delay-dependent manner. This dependence will cause significant performance degradation due to large variation in the pulse power in the data stream.

In this paper, we propose a slow-light method that avoids large power variations in the delayed pulses. Our method uses two widely separated absorption resonances that are generated by SBS and achieves slow light for signal pulses whose frequency lies in between two absorption lines. The resonances are due to anti-Stokes absorption when the SBS process is pumped by a two-frequency pump beam. This method also has a large bandwidth suitable for shorter

pulses, even though the absorption lines have a narrow linewidth (~ 30 MHz in standard optical fiber SMF-28e). Our method is similar to the one that was recently demonstrated using two absorption resonances in atomic gases [21, 22].

This paper is organized as follows. In the next section, we present a theoretical analysis of the method. In Section 3, we describe our experiment and present the experimental results. Section 4 concludes the paper.

2. Theory

Our method to achieve nearly transparent slow light in optical fibers is to use two Lorentzian-shaped absorption resonances that are generated by stimulated Brillouin scattering. To achieve an absorption doublet, a two-frequency continuous-wave (CW) laser beam (of angular frequencies $\omega_p \pm \Delta$) can be used to pump an optical fiber along $-z$ -direction, giving rise to absorbing resonances at anti-Stokes frequencies $\omega_p \pm \Delta + \Omega_B$ due to the process of electrostriction, where Ω_B is the Brillouin frequency shift in the fiber. A counterpropagating beam (along the $+z$ -direction) experiences these resonances in the vicinity of the anti-Stokes frequencies. It is straightforward to obtain a two-frequency CW pump laser field from a single CW laser using carrier-frequency-suppression amplitude modulation [23, 24]. For simplicity, we assume the two resonances have the same characteristics except for their resonant frequencies. The complex linear susceptibility for such a medium with two Lorentzian-shaped absorption resonances is given by [24]

$$\chi = i \frac{cn_0\alpha_0}{\omega} \left[\frac{1}{1 - i(\delta + \Delta)/\gamma} + \frac{1}{1 - i(\delta - \Delta)/\gamma} \right], \quad (1)$$

where $\delta = \omega - \omega_0 = \omega - (\omega_{20} + \omega_{10})/2$, $\Delta = (\omega_{20} - \omega_{10})/2$, ω_{10} and ω_{20} are the line centers of the two absorption resonances, α_0 is the line-center absorption coefficient, γ is the half-width at half-maximum of the resonances, n_0 is the background refractive index, and c is the speed of light in vacuum. The refractive index associated with these resonances is given by

$$n(\delta) = n_0 + \frac{1}{2n_0}\chi = n_0 + i \frac{c\alpha_0}{2\omega} \left[\frac{1}{1 - i(\delta + \Delta)/\gamma} + \frac{1}{1 - i(\delta - \Delta)/\gamma} \right]. \quad (2)$$

The intensity absorption coefficient is then given by

$$\alpha(\delta) = \frac{\omega}{c} \text{Im} \left(\frac{\chi}{n_0} \right) = \alpha_0 \left[\frac{1}{1 + (\delta + \Delta)^2/\gamma^2} + \frac{1}{1 + (\delta - \Delta)^2/\gamma^2} \right]. \quad (3)$$

The additional time delay experienced by an optical pulse (of carrier frequency of ω_0) propagating through a material of length L is given by

$$T_{del} = \frac{L}{c} (n_g - n_0) = \frac{\alpha_0 L}{\gamma} \frac{(\Delta/\gamma)^2 - 1}{[1 + (\Delta/\gamma)^2]^2}, \quad (4)$$

where $n_g = (n + \omega dn/d\omega)|_{\omega=\omega_0}$ is the group index evaluated at ω_0 . When $\Delta > \gamma$, $T_{del} > 0$. This shows that the pulse experiences delay when the two absorption resonances are widely separated. The intensity attenuation parameter at $\delta = 0$ is given by $A_0 = \alpha(\delta = 0)L = 2\alpha_0 L / (1 + \Delta^2/\gamma^2)$ and it is related to T_{del} by

$$T_{del} = \frac{A_0}{2\gamma} \frac{(\Delta/\gamma)^2 - 1}{(\Delta/\gamma)^2 + 1}. \quad (5)$$

Figures 1(a) and 1(b) show an example of the refractive index and absorption associated with the two absorption resonance lines where the line separation is set at $\Delta = 3\gamma$. The normal

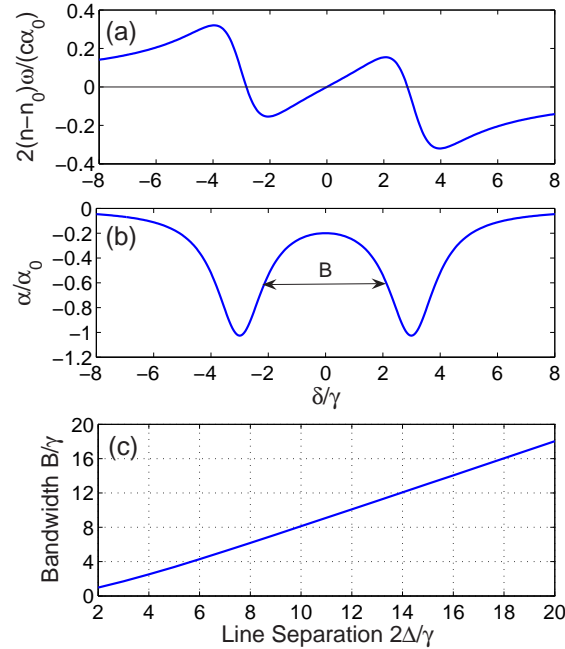


Fig. 1. (a) Refractive index (b) absorption coefficient and (c) slow light bandwidth for the absorption doublet. In (a) and (b), $\Delta = 3\gamma$. The slow light bandwidth (FWHM) B is determined from the absorption spectrum as illustrated in (b).

dispersion between the resonances at $\delta = 0$ is used to increase the group index so as to achieve slow light.

The FWHM bandwidth B of the slow light can be estimated from Eq. (3) by calculating the spectral span across the two half-height points between the absorption valley and two peaks, as illustrated in Fig. 1(b). Figure 1(c) shows the slow-light bandwidth as a function of the line separation 2Δ . It is seen that the bandwidth increases linearly with the line separation. However, the increase of the line separation reduces the slow light delay in a nonlinear manner as shown in Eq. (4). We examine the delay-bandwidth product $T_{del}B$ and find there exists an optimal line separation that gives rise to the maximum delay-bandwidth product, as shown in Fig. 2(a). The delay falls off only slowly for large line separations. This demonstrates that it is possible to obtain large bandwidths using the proposed method.

The advantage of our method in achieving nearly transparent slow light is manifested in the comparison with that based on a single SBS gain resonance of the same bandwidth B . The slow light delay for the latter is simply given by $T_{del} = G_0/B$ [11, 25], where G_0 is the gain parameter. If we require the two methods achieve the same pulse delay, then we have

$$\frac{G_0}{A_0} = \frac{B (\Delta/\gamma)^2 - 1}{2\gamma (\Delta/\gamma)^2 + 1}. \quad (6)$$

Figure 2(b) shows G_0/A_0 as a function of the line separation 2Δ . It is seen that A_0 is smaller than G_0 when $2\Delta/\gamma > 4.53$, indicating a much smaller pulse power change in the proposed method. For example, when $2\Delta/\gamma = 14$, the signal attenuation (in dB) for the absorption-doublet method is only $\sim 1/6$ of the gain (in dB) for the corresponding gain-singlet method.

As in the gain-singlet SBS slow light, the delayed signal pulse acquires distortion and the main contribution to the pulse distortion is the frequency-dependent gain or attenuation, which

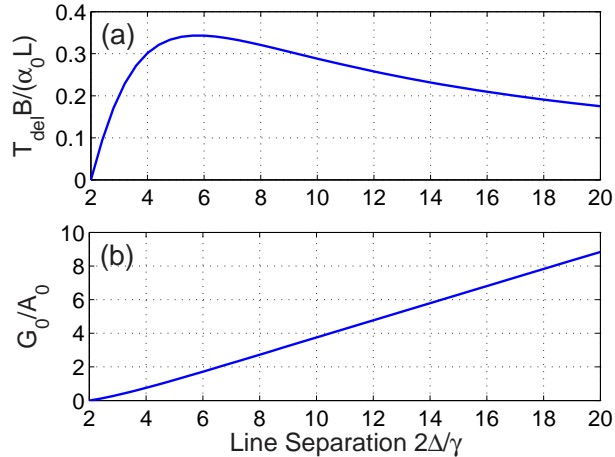


Fig. 2. (a) Delay-bandwidth product as a function of the line separation for the absorption-doublet slow-light method. (b) Comparison in signal pulse power variations between the gain-singlet and the absorption-doublet slow light at the same delay and bandwidth.

gives rise to a pure imaginary group-velocity-dispersion coefficient. The third-order dispersion, which comes only from the real part of the refractive index, is usually negligible. In the case of negligible third-order dispersion, for a Gaussian-shaped input pulse (intensity $\propto \exp[-(t/\tau_{in})^2]$) with center frequency tuned at ω_0 , the output pulse width is given by

$$\tau_{out} = \left[\tau_{in}^2 + \frac{A_0}{\gamma^2} \frac{3(\Delta/\gamma)^2 - 1}{[1 + (\Delta/\gamma)^2]^2} \right]^{1/2}. \quad (7)$$

From Eqs. (5) and (7), it is seen that the signal pulse is always broadened under conditions for which the pulse experiences delay ($\Delta > \gamma$). The slow-light pulse distortion could be minimized using distortion-compensation methods [24, 26].

The above theoretical analysis assumes an ideal Lorentzian shaped anti-Stokes absorption spectrum. In reality, the absorption spectrum may deviate from the ideal Lorentzian shape due to inhomogeneous broadening or multiple acoustic modes. Therefore, the absorption and dispersion characteristics can be different from the ideal Lorentzian line case. However, as long as the distortion in the absorption spectrum is not significant, the analytical results presented above will give a good estimation of the slow light characteristics with realistic absorption spectra.

Due to strong filtering and dispersive effect with slow light propagation, optical pulses with sharp edges can be significantly distorted, causing ambiguity in determining slow light delay. To avoid this ambiguity, pulses with smooth edges (e.g., Gaussian pulses) are usually used in slow light studies. A recent study on pulse propagation through a single-resonance slow-light medium has shown that arbitrarily shaped pulses tend to acquire a nearly Gaussian shape [27]. For these reasons and theoretical convenience as well, we only consider Gaussian shaped pulses in both the theoretical analysis and the experimental study.

3. Experiment and results

An absorption-doublet with an adjustable frequency separation 2Δ is realized by pumping a room-temperature highly nonlinear optical fiber (HNLF) with a bichromatic laser field, which is obtained via carrier-frequency-suppression amplitude modulation of a CW single-frequency laser field [23, 24]. The doublet spacing 2Δ is adjusted by changing the frequency of the voltage driving the modulator and the slow light delay is adjusted by changing the pump power.

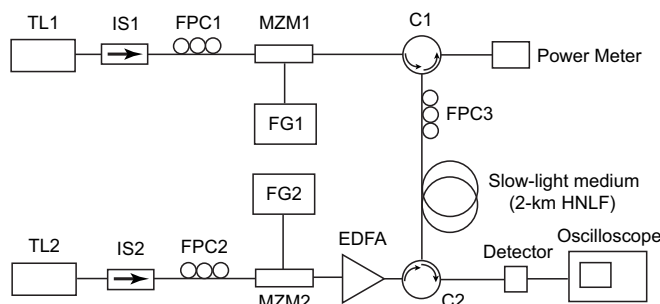


Fig. 3. Experiment setup based on two anti-Stokes absorption lines in an optical fiber via stimulated Brillouin scattering. TL1, TL2: tunable lasers; IS1, IS2: isolators; FPC1, FPC2, FPC3: fiber polarization controllers; MZM1, MZM2: Mach-Zehnder modulators; FG1, FG2: function generators; EDFA: Erbium-doped fiber amplifier; C1, C2: circulators.

The experimental setup is shown schematically in Fig. 3. Two 1550-nm narrow-linewidth tunable lasers (TL1 and TL2) are used to produce signal pulses and the pump beam, respectively. A bichromatic pump beam is produced by passing the single-frequency CW laser beam generated by TL2 (angular frequency ω_p) through modulator MZM2, which is driven by a sinusoidal voltage of angular frequency Δ . The bias voltage applied to MZM2 is chosen to suppress the carrier frequency, resulting in a beam with two frequencies ($\omega_p \pm \Delta$). This beam is amplified by an erbium-doped fiber amplifier (EDFA) and routed via circulator C2 to pump a 2-km-long HNLF (OFS Denmark). For this fiber, we measure an SBS absorption linewidth (full-width at half-maximum) of $\gamma/\pi \sim 50$ MHz. After passing through the slow-light medium, the beam is routed out of the system via circulator C1 and monitored by a power meter.

The signal pulses are produced from a laser beam generated by TL1. The beam passes through an isolator, a fiber polarization controller, and modulator MZM1, producing pulses with carrier frequency ω_c . The pulses enter the 2-km-long HNLF via circulator C1 and counterpropagate with respect to the bichromatic pump beam in the fiber. The slow-light-delayed and attenuated pulses are routed out of the system via C2, detected by a fast photoreceiver, and displayed on a digital oscilloscope. The frequency difference between TL1 and TL2 is tuned so that the pulse carrier frequency is set precisely to the center between the two anti-Stokes absorption resonances, i.e., $\omega_c = \omega_p + \Omega_B$, where $\Omega_B/2\pi = 9.6$ GHz is the Brillouin frequency shift for the HNLF. Fiber polarization controllers FPC1 and FPC2 are used to maximize the transmissions through the Mach-Zehnder modulators, and FPC3 is used to maximize the SBS slow-light delay experienced by the signal pulses.

Figure 4 shows the experimental results when the absorption line separation is set at 200 MHz, i.e., $2\Delta/\gamma = 8$. The input signal pulses have a pulsewidth (FWHM) of about 9 ns. In the left column of the figure, we show both the delayed and un-delayed pulse intensities in the same scale for total pump powers of 5 dBm, 10 dBm, and 13 dBm (from top to bottom). The right column of the figure shows the corresponding power absorption spectra (obtained by measuring the transmission of a CW signal beam through the slow light medium). It is seen that the pulse delay increases with the pump power, and that the pulse power decreases as the pump power increases due to increased absorption. The signal pulse is delayed by about 2.6 ns and is attenuated by 4.8 dB at the pump power of 13 dBm. To achieve the same amount of delay using a single SBS amplifying resonance of the same bandwidth, the signal pulse will acquire an amplification of 12.3 dB. This demonstrates that the proposed slow light method can greatly reduce the output pulse power variation and therefore enable nearly transparent slow light.

By fitting the pulse traces shown in Fig. 4 with a Gaussian function, the pulse delay, power

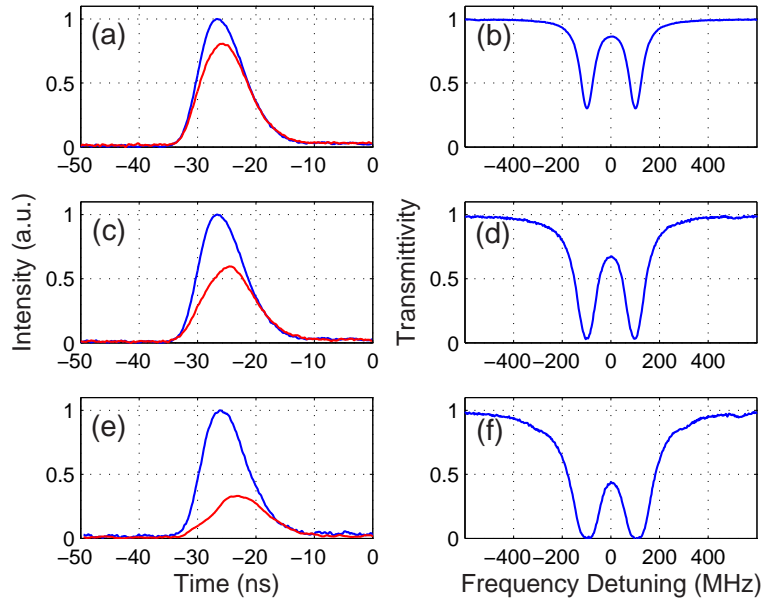


Fig. 4. Experimental results with two anti-Stokes absorption lines. Each line has a linewidth of $2\gamma/2\pi = 50$ MHz and the line separation is $2\Delta/2\pi = 200$ MHz. (a),(c),(e): Traces of delayed (shown in red) and un-delayed (shown in blue) signal pulses at a pump power of 5 dBm, 10 dBm, and 13 dBm, respectively; (b), (d), (f): Power absorption spectra measured with a CW signal beam at the corresponding pump powers.

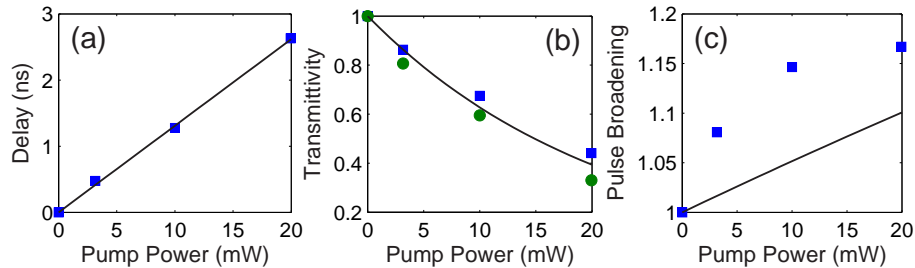


Fig. 5. (a) Pulse delay, (b) power transmittivity, and (c) pulse broadening as a function of the pump power. The data points shown in squares are obtained by Gaussian fitting the pulses traces in Fig. 4. The data points shown in circles are the zero-detuning transmittivity from Fig. 4. The solid line in (a) is a line fit of the measured delay as a function of the pump power, which provides a parameter to obtain the theoretical results of transmittivity and pulse broadening that are shown in (b) and (c) as solid curves.

transmission and pulse broadening are obtained and shown in Fig. 5 as solid squares. The pulse broadening is defined as the ratio of the delayed pulse width to the undelayed pulse width. The transmittivities measured with a CW signal beam at zero-detuning (from Figs. 4(b)(d)(f)) are also shown in Fig. 5(b) as solid circles. From a linear fit of the measured delay versus the pump power (solid line in Fig. 5(a)) and using Eqs. (5) and (7), theoretical predictions of power transmission and pulse broadening are obtained and shown as solid curves in Figs. 5(b) and 5(c). The measured power transmission data agree well with the theoretical ones. The large discrepancy between the measured pulse broadening and the theoretical prediction may

be due to the fact that the input pulses are far from ideal Gaussian pulses. Nonetheless, the measured pulse broadening is small for the 9-ns input pulse because of the relative large slow light bandwidth (~ 150 MHz as estimated from Fig. 1(c) and Fig. 4(b)).

In order to achieve a large slow-light delay, one needs to increase the attenuation parameter A_0 at a given line separation (see Eq. (5)). However, to obtain large anti-Stokes absorption by increasing the pump power or the fiber length will cause the build up of the Stokes fields that are downshifted from the pump frequencies by the Brillouin frequency shift. The energy transfer from the pump beam to the counterpropagating Stokes beam reduces the pump power that can pass through the fiber and hence the anti-Stokes absorption. This problem may be obviated by a multi-stage slow-light approach [13], where a filter can be inserted between two adjacent stages to attenuate the Stokes field. This approach is equivalent to putting multiple filters along the fiber length to suppress the build up of Stokes fields without affecting the pump and the signal fields.

4. Conclusion

We have described a slow-light method that is based on two widely separated absorption resonances. It is implemented in a room-temperature optical fiber that is pumped by a bichromatic laser beam, which induces an absorption doublet via anti-Stokes stimulated Brillouin scattering. Compared to SBS slow light based on a single SBS gain resonance, the proposed method has the advantages of easily controllable large bandwidths and smaller variation in pulse power, indicating that better system performance can be achieved with the proposed method. This approach can be extended to achieve broader bandwidths using spectrally broadened pump light [15, 28, 29] and smaller pulse distortion by tailoring the shape of the absorption lines [24, 26].

Acknowledgment

We gratefully acknowledge the financial support of the DARPA DSO Slow-Light Program.